

Identifying Entanglement Using Quantum Ghost Interference and Imaging

Milena D'Angelo,^{1,*} Yoon-Ho Kim,^{2,†} Sergei P. Kulik,^{1,‡} and Yanhua Shih¹

¹*Department of Physics, University of Maryland, Baltimore County, Baltimore, Maryland, 21250, USA*

²*Department of Physics, Pohang University of Science and Technology (POSTECH), Pohang, 790-784, Korea*

(Received 20 August 2003; published 8 June 2004)

We report a quantum interference and imaging experiment which allows identifying the entanglement in momentum and position variables of a two-photon system. The measurements show indeed that the uncertainties in the sum of momenta and in the difference of positions of the entangled two-photon satisfy both EPR inequalities $\Delta(k_1 + k_2) < \min(\Delta k_1, \Delta k_2)$ and $\Delta(x_1 - x_2) < \min(\Delta x_1, \Delta x_2)$. These two inequalities, together, represent a nonclassicality condition. Our measurements provide a direct way to distinguish between quantum entanglement and classical correlation in continuous variables for systems of pairs of photons.

DOI: 10.1103/PhysRevLett.92.233601

PACS numbers: 42.50.Xa, 03.65.Ud, 42.50.St, 42.65.Lm

The concept of multiparticle quantum entanglement, one of the most surprising consequences of quantum mechanics, was introduced in the very early days of quantum theory [1,2]. Since the development of spontaneous parametric down-conversion (SPDC) as an efficient source of two-photon entangled states in the 1980's [3], many experiments have been realized to exhibit and, afterwards, to exploit the very surprising quantum effects of entangled states for secure communication, information processing, and metrology applications [4].

Some of the most intriguing effects of two-photon entanglement in SPDC are quantum “ghost” interference and imaging [5,6]. These effects are of great importance in potential applications such as quantum metrology and lithography [7–9]. Recently, it has been claimed that the two-photon ghost image can be achieved using pairs of classically \mathbf{k} -vector correlated optical pulses [10]. Reference [10], therefore, raises interesting questions about fundamental issues of quantum theory, namely: (i) To what extent can quantum entanglement in continuous variables be simulated with classically correlated systems, and (ii) can we experimentally distinguish them?

In this Letter, we report an experiment which sheds light on these two tightly related questions. Our idea is to exploit quantum interference-imaging effects to verify experimentally the Einstein-Podolsky-Rosen (EPR)-type inequalities, which allow distinguishing quantum entanglement from classical correlation in momentum and/or position variables, for two-photon systems. By analyzing the results of a two-photon interference and imaging experiment, we show quantitatively that *entangled* two-photon pairs exhibit both momentum-momentum and position-position EPR-type correlations, which are stronger than any classical correlation. In contrast, pairs of particles having a perfect *classical correlation* in momentum (or position) cannot exhibit any correlation in position (or momentum), due to the uncertainty principle. Our experiment, therefore, shows that entanglement in momentum and position variables for two-photon sys-

tems can be verified experimentally and suggests that the degree of entanglement can be quantified through the EPR inequalities. This result is of particular interest, since it represents a “Bell’s inequality” for continuous variables, for two-photon systems.

As pointed out by EPR [2], the most peculiar characteristic of entanglement is its independency on the selected basis: Entanglement in momentum automatically implies entanglement in position. Indeed, in EPR notation [2], the quantum state of an entangled pair of particles can be written as

$$\Psi(x_1, x_2) = \int u_p(x_1)\psi_p(x_2) dp = \int v_x(x_1)\phi_x(x_2) dx,$$

where x_1 (x_2) is the variable used to describe particle 1 (particle 2), $u_p(x_1)$ [$\psi_p(x_2)$] is the momentum eigenfunction for particle 1 (particle 2), and $v_x(x_1)$ [$\phi_x(x_2)$] is the corresponding position eigenfunction obtained by Fourier transform of $u_p(x_1)$ [$\psi_p(x_2)$].

As suggested by EPR, an important consequence of entanglement appears explicitly by considering the case in which $u_p(x_1)$ [$\psi_p(x_2)$] is a plane wave. Indeed, in this case, the EPR-entangled state assumes an interesting form:

$$\begin{aligned} \Psi(x_1, x_2) &= \frac{1}{2\pi\hbar} \int \delta(p_1 + p_2) e^{ip_1 x_1/\hbar} e^{ip_2 x_2/\hbar} dp_1 dp_2 \\ &= \delta(x_1 - x_2), \\ \bar{\Psi}(p_1, p_2) &= \frac{1}{2\pi\hbar} \int \delta(x_1 - x_2) e^{-ip_1 x_1/\hbar} e^{-ip_2 x_2/\hbar} dx_1 dx_2 \\ &= \delta(p_1 + p_2). \end{aligned} \quad (1)$$

An EPR-entangled pair of particles is therefore characterized by both uncertainties $\Delta(p_1 + p_2) = 0$ and $\Delta(x_1 - x_2) = 0$. In a nonmaximally entangled system, these uncertainties may be different from zero, nevertheless they may still satisfy both inequalities:

$$\begin{aligned}\Delta(p_1 + p_2) &< \min(\Delta p_1, \Delta p_2), \\ \Delta(x_1 - x_2) &< \min(\Delta x_1, \Delta x_2).\end{aligned}\quad (2)$$

An entangled pair of particles is indeed described in such a way that both the sum of the momenta and difference in the positions are known with a high degree of accuracy even if both the momentum and position of each particle are completely undefined [2]. An entangled pair of particles can then be described only as a whole (i.e., as a two-particle [11]). This result is an immediate consequence of the *coherent superposition* of *two-particle amplitudes*, which cannot be achieved by any system of classically correlated pairs of particles, as discussed in more detail later.

We propose Eqs. (2) as a nonclassicality condition for identifying entanglement in momentum and position variables, for microscopic bipartite systems. We report an experimental verification of Eq. (2) which exploits quantum ghost interference and imaging effects of entangled two-photon pairs. We measure $\Delta(k_1 + k_2)$ from a quantum interference experiment and $\Delta(x_1 - x_2)$ from a quantum imaging experiment, both realized using the same SPDC source. To the best of our knowledge, a direct quantitative verification of Eqs. (2) for the two-photon system, i.e., for real momentum and position variables, has not been reported in literature [12].

Let us first examine whether SPDC two-photon pairs would really exhibit EPR-type entanglement. Under the assumption that the pump beam is a plane wave and the transverse dimensions of the pump beam and the down-conversion crystal are much bigger than the wavelengths of the photons, the quantum state of the SPDC two-photon pairs can be written as [11,13]

$$|\Psi\rangle = \sum_{s,i} \delta(\omega_s + \omega_i - \omega_p) \delta(\mathbf{k}_s + \mathbf{k}_i - \mathbf{k}_p) a_s^\dagger a_i^\dagger |0\rangle, \quad (3)$$

where ω_j and \mathbf{k}_j (with $j = s, i, p$) are the frequency and wave vector of the signal (s), idler (i), and pump (p), respectively, and a_s^\dagger (a_i^\dagger) is the creation operator for the signal (idler) photon. Since in this Letter we are interested only in the transverse correlation of the entangled two-photon pairs [13], the quantum state used in our experiment is indeed very close to the one of the original EPR-entangled pairs. Verification of the EPR inequalities of Eq. (2) should then be possible through adequate experiments realized with this source.

A schematic of the experimental setup can be seen in Fig. 1. The 351.1 nm line of an argon ion laser is used to pump a beta barium borate crystal cut for type-II collinear degenerate SPDC. Pairs of orthogonally polarized signal and idler photons at central wavelength $\lambda_i = \lambda_s = 702.2$ nm, which are entangled in momentum [Eq. (3)], emerge from the crystal almost collinearly with the pump laser. After the crystal, the pump laser beam is separated from the SPDC beam by a quartz dispersion prism. A polarization beam splitting Thompson prism separates

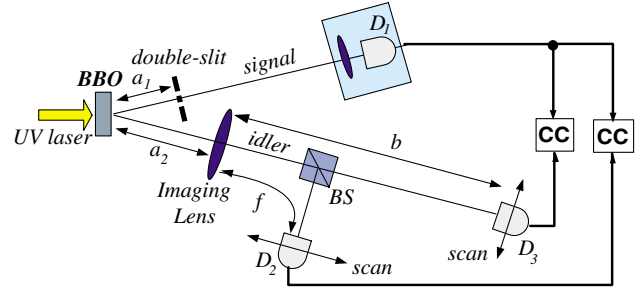


FIG. 1 (color online). Schematic of the experimental setup. Ghost interference is observed in the focal plane of the lens (Fourier transform plane, or momentum space) to measure the momentum-momentum correlation, while the ghost image is observed in the two-photon imaging plane to measure the position-position correlation. The double slit has width $a = 0.165$ mm and slit distance $d = 0.4$ mm. The imaging lens has focal length $f = 510$ mm. Relevant distances in this experiment are $a_1 = 32.5$, $a_2 = 46.5$, and $b = 142$ cm.

the copropagating signal and idler into two separate spatial modes. The signal photon propagates through a double slit toward a detector package (D_1) consisting of a collection lens (500 mm focal length) and a single photon detector placed in its focus. The idler photon propagates freely before being collected by the imaging lens ($f = 510$ mm). A 50-50 beam splitter (BS) is inserted after the lens. The reflected and transmitted photons are then detected by single photon detectors D_2 and D_3 , respectively. Each of them is mounted on an encoder driver to scan its own transverse plane. A spectral filter centered at 702.2 nm with 3 nm bandwidth precedes each detector. The output pulses of the detectors are sent to a coincidence circuit (CC). Coincidences are measured between D_1 and D_2 and between D_1 and D_3 .

This setup therefore allows one to measure both ghost interference diffraction and ghost image patterns of the double slit [5,6]. Indeed, the *coherent superposition* of biphoton amplitudes allows exploiting the momentum-momentum correlation to obtain an image (position-position correlation) by simply changing the observation plane (D_3 , instead of D_2) [13–15]. The results are shown in Fig. 2. The single counts on both D_2 and D_3 , which are scanned in the transverse direction, are fairly constant. The single counting rate of D_1 , when the detector scans the focal plane of the collection lens, did not show any interference fringes as well: Only a wide bell-shaped pattern was observed. This result is due to the fact that biphotons are generated with all possible momenta \mathbf{k}_i and \mathbf{k}_s such that $\mathbf{k}_s + \mathbf{k}_i = \mathbf{k}_p$ is satisfied. In our experiment, the divergence of the SPDC beam $\Delta(\theta)$, which takes into account the filter bandwidth, the dispersion in the crystal, and the phase matching condition, is such that $\Delta(\theta) \approx 2.6$ mrad $\gg \lambda/d$, where $d = 0.4$ mm is the distance between the slits and $\lambda = 702.2$ nm is the central wavelength of the SPDC photons. Under this condition, the first order interference-diffraction pattern on D_1 is simply washed out.

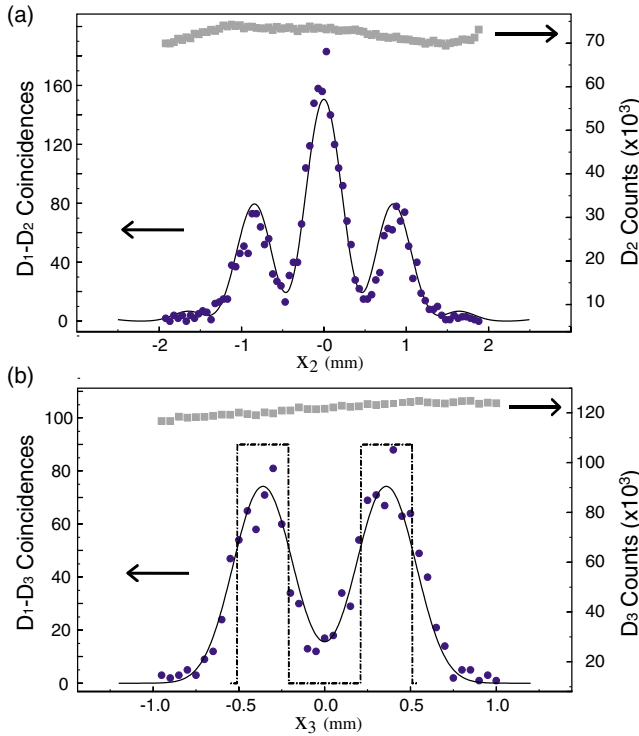


FIG. 2 (color online). Experimental data. (a) Ghost interference-diffraction pattern. (b) Ghost image pattern. $\Delta(\mathbf{k}_1 + \mathbf{k}_2)$ and $\Delta(\mathbf{r}_1 - \mathbf{r}_2)$ are evaluated from each of the fitting curves (solid lines). The squares are single counts; the dots are coincidence counts.

It is, however, possible to observe a ghost interference-diffraction pattern when counting coincidences between D_1 and D_2 (D_1 is fixed and D_2 is scanned in the focal plane of the imaging lens) and to observe a ghost image pattern in coincidences between D_1 and D_3 (D_1 is, again, fixed and D_3 is scanned in the image plane).

For ghost interference-diffraction measurement, the detector package D_1 plays the role of a pointlike detector. As shown in Ref. [5], we expect the coincidence counting rate to be

$$R_c(x_2) \propto \text{sinc}^2[x_2 \pi a / (\lambda f)] \cos^2[x_2 \pi d / (\lambda f)], \quad (4)$$

where x_2 is the transverse position of detector D_2 in the focal plane of L_2 . Figure 2(a) shows the ghost interference measurement. The continuous line in Fig. 2(a) is a fitting of the experimental data, which takes into account the finite size of the detectors, the divergence of the pump, and the less-than-perfect correlation between signal and idler. It is well known that the visibility of the interference pattern $\{\propto 1 + V \cos[2x_2 \pi d / (\lambda f_2)]\}$ is related to the degree of transverse coherence of the source. We exploit this effect to evaluate the less-than-perfect transverse correlation between signal and idler photons:

$$\Delta(k_{x_s} + k_{x_i}) = 2.5 \pm 0.6 \text{ mm}^{-1}.$$

From the divergence of the SPDC beam $\Delta(\theta)$ mentioned 233601-3

above, we evaluate $\Delta k_{x_j} \approx 23 \text{ mm}^{-1}$, for $j = i, s$. So the ghost interference/diffraction experiment demonstrates that

$$\Delta(k_{x_s} + k_{x_i}) \ll \min(\Delta k_{x_i}, \Delta k_{x_s}),$$

for our SPDC source.

In a similar way, we obtain $\Delta(x_s - x_i)$ by studying the ghost image obtained by measuring coincidences between D_1 and D_3 [see Fig. 2(b)]. To observe a ghost image, the two-photon Gaussian thin lens equation, $1/s_i + 1/s_o = 1/f$, where $s_i = b$ and $s_o = a_1 + a_2$, must be satisfied [6]. In the ideal situation, the detector package D_1 is a perfect bucket detector, which detects any signal photon that has not been stopped by the double slit. The role of the double slit is then to measure the localization of the signal photon with an uncertainty $\Delta(x_s)$, equal to $a + d$. In the ideal case, counting coincidences between D_1 and D_3 , we would obtain two rectangles of width $a' = ma$, and center-to-center distance $d' = md$, where $m = s_i/s_o$ is the magnification. In our case $m = 1.8$, $a = 0.165 \text{ mm}$, $d = 0.4 \text{ mm}$, and the corresponding ideal result ($a' = 0.297 \text{ mm}$, $d' = 0.72 \text{ mm}$) is plotted as a dashed line in Fig. 2(b). To take into account a more realistic situation, we fit the data with the convolution of the double slit with a Gaussian function that takes into account the finite size of D_2 . The comparison of the resulting fitting curve with the theoretical result, dashed line in Fig. 2(b), allows one to evaluate $\Delta(x_s - x_i)$ as the difference between the variances of the two curves:

$$\Delta(x_s - x_i) = 0.11 \pm 0.02 \text{ mm} \ll \Delta x_s.$$

Note that the center-to-center distance between the bell-shaped fitting curve and the two rectangles is exactly the same. The imperfect correlation in position is evidently smaller than the distance between the two slits.

Both EPR inequalities introduced in Eqs. (2) are then satisfied by the momentum and position variables measured on the entangled two-photon pairs emitted by SPDC. As we mentioned earlier, this result is a direct consequence, if not the definition, of quantum correlation: Particles that are entangled in momentum are automatically entangled in position. Only entangled two-particle-two-photon pairs can satisfy both inequalities.

An interesting way of understanding this result is the following. An entangled state such as the one given in Eq. (1) [and Eq. (3)], can be factored [11] by introducing the variables $p_1 + p_2$ and $(p_1 - p_2)/2$. The corresponding Fourier-conjugate variables are $(x_1 + x_2)/2$ and $x_1 - x_2$, respectively. Since $p_1 + p_2$ and $x_1 - x_2$ are not Fourier-conjugate variables, Eqs. (2) can definitely be true simultaneously. For this same reason, also the product of the two uncertainties can be smaller than 1.

Let us now consider a statistical mixture of pairs of quanta classically correlated in momentum. An example of such a source is given by a pair of bounded identical 233601-3

guns which emit (quantum) particles while rotating simultaneously, in such a way that the momenta of the two particles are always equal in modulus but with opposite direction. Each pair of independent but correlated particles, fired at a certain angle at a given time, may be described by

$$|\Psi_j\rangle_{12} = a_1^\dagger(\mathbf{k}_j)a_2^\dagger(-\mathbf{k}_j)|0\rangle.$$

If each pair of particles has (non-negative) probability $P(\mathbf{k}_j)$ of being emitted by the source, the resulting incoherent statistical mixture is described by the following density matrix:

$$\rho_{12} = \sum_{\mathbf{k}_j} P(\mathbf{k}_j) |\Psi_j\rangle_{12} \langle\Psi_j| = \sum_{\mathbf{k}_j} P(\mathbf{k}_j) \rho_1^j \otimes \rho_2^j, \quad (5)$$

where $\rho_1^j = |\mathbf{k}_j\rangle_{11}\langle\mathbf{k}_j|$ and $\rho_2^j = |-\mathbf{k}_j\rangle_{22}\langle-\mathbf{k}_j|$ are the density matrices for particles 1 and 2, respectively, belonging to the j th pair. It is well known that, for each particle to propagate with such a perfectly well-defined momentum, the transverse dimension of the source has to be infinite [16,17]. Therefore, pairs of particles with a perfect momentum-momentum correlation do not exhibit any position-position correlation. In the more realistic case of finite transverse dimension of the source, the position-position correlation improves at the expense of the momentum-momentum correlation: Each particle is always diffracted independently. In general, any attempt to improve the classical correlation in one variable inevitably worsens the correlation in the other. Thus, a system of classically correlated particles can never satisfy both EPR inequalities [Eqs. (2)].

In conclusion, any source of classically correlated pairs of quanta (i) can never achieve perfect correlation in both momentum and position variables, and (ii) can never satisfy the pair of EPR inequalities [Eqs. (2)].

In summary, we have experimentally demonstrated that SPDC two-photon pairs satisfy both EPR inequalities of Eqs. (2). In doing so, we have shown that entangled particles exhibit almost perfect correlation in both momentum and position variables. Classically correlated pairs of particles cannot exhibit such behavior. The measurement described in this Letter thus provides a direct way to distinguish between quantum entanglement and classical correlation in momentum and/or position variables, for two-photon systems. An important practical consequence is that only the nonlocal correlation implicit in entangled systems allows one to “overcome” the usual diffraction limit and to obtain super-resolved images, as proposed and demonstrated in Refs. [8,9,17]. Furthermore, our experiment shows that a distinction between classically correlated and quantum entangled systems, in momentum and/or position variables, can be realized experimentally through the study of ghost imaging-type

experiments [18]. This is a quite different approach with respect to Bell’s inequality and may represent an extension of Bell’s inequality in optics.

The authors thank M. H. Rubin and V. Protopopescu for helpful comments and discussions. This work was supported, in part, by NASA-CASPR program, NSF, and ONR. Y.H.K. also acknowledges support from the Korea Research Foundation (KRF-2003-070-C00024).

*Electronic address: dmilenal@umbc.edu

†Electronic address: yoonho@postech.ac.kr

‡Permanent address: Department of Physics, Moscow State University, Moscow, Russia.

- [1] E. Schrödinger, in *Quantum Theory and Measurement*, edited by J.A. Wheeler and W.H. Zurek (Princeton University Press, New York, 1983).
- [2] A. Einstein, B. Podolsky, and N. Rosen, *Phys. Rev.* **47**, 777 (1935).
- [3] D. N. Klyshko, *Photon and Nonlinear Optics* (Gordon and Breach Science, New York, 1988).
- [4] J. P. Dowling and G. J. Milburn, quant-ph/0206091; A. Migdall, *Phys. Today* **52**, No. 1, 41 (1999).
- [5] D. V. Strekalov *et al.*, *Phys. Rev. Lett.* **74**, 3600 (1995).
- [6] T. B. Pittman *et al.*, *Phys. Rev. A* **52**, R3429 (1995).
- [7] V. Giovannetti, S. Lloyd, and L. Maccone, *Phys. Rev. A* **65**, 022309 (2002); Y. Shih (unpublished).
- [8] A. N. Boto, P. Kok, D. S. Abrams, S. L. Braunstein, C. P. Williams, and J. P. Dowling, *Phys. Rev. Lett.* **85**, 2733 (2000).
- [9] M. D’Angelo, M. V. Chekhova, and Y. Shih, *Phys. Rev. Lett.* **87**, 013602 (2001).
- [10] R. S. Bennink, S. J. Bentley, and R. W. Boyd, *Phys. Rev. Lett.* **89**, 113601 (2002).
- [11] M. H. Rubin, D. N. Klyshko, Y. H. Shih, and A. V. Sergienko, *Phys. Rev. A* **50**, 5122 (1994).
- [12] A similar nonclassicality relation has been verified experimentally for an OPO [Z. Y. Ou, S. F. Pereira, H. J. Kimble, and K. C. Peng, *Phys. Rev. Lett.* **68**, 3663 (1992)]. The quantities measured in the experiment are the spectral components of the quadrature-phase amplitudes (phase and intensity) of the signal and idler beams.
- [13] M. H. Rubin, *Phys. Rev. A* **54**, 5349 (1996).
- [14] M. H. Rubin, quant-ph/0303188.
- [15] A. Gatti, E. Brambilla, and L. A. Lugiato, *Phys. Rev. Lett.* **90**, 133603 (2003)
- [16] D. Bedford and F. Selleri, *Lett. Nuovo Cimento* **42**, 325 (1985); M. J. Collet and R. Loudon, *Nature (London)* **326**, 671 (1987).
- [17] Y.-H. Kim and Y. H. Shih, *Found. Phys.* **29**, 1849 (1999).
- [18] Cancellation of first order effects is a prerequisite for making this distinction since quantum ghost interference-imaging phenomena are second order effects. Also, two independent measurements are required: one in momentum space (Fourier transform plane) and another one in position space (image plane).